Performance on molecules, surfaces, and solids of the Wu-Cohen GGA exchange-correlation energy functional

Fabien Tran, Robert Laskowski, Peter Blaha, and Karlheinz Schwarz
Institute of Materials Chemistry, Vienna University of Technology, Getreidemarkt 9/165-TC, A-1060 Vienna, Austria
(Received 13 November 2006; revised manuscript received 15 January 2007; published 30 March 2007)

We present the results of Kohn-Sham calculations on molecules, surfaces, and solids which were obtained using a recently proposed exchange-correlation energy functional [Z. Wu and R. E. Cohen, Phys. Rev. B **73**, 235116 (2006)]. The Wu-Cohen (WC) functional, like the well-known PBE functional [J. P. Perdew *et al.*, Phys. Rev. Lett. **77**, 3865 (1996)], is of the generalized gradient approximation form and was derived from the homogeneous electron gas and mathematical relations obeyed by the exact functional. The results on molecular systems show that among the functionals we tested, PBE remains superior for the energetics of covalent and noncovalent bonds. While this is not too surprising for noncovalent bonds due to the very good performance of PBE, unfortunately this holds also for covalent bonds, where PBE is a functional of rather poor quality. Calculations on transition-metal surfaces show that WC improves over local-density approximation (LDA) and PBE for the surface formation energy of 3*d* elements, while LDA is the best for heavier elements. In most cases, the lattice constant of solids as determined by the WC functional is in between the LDA and PBE results and on average closer to experiment. We show for each group of compounds which functional performs best and provide trends. In the particular case of lattice constants whose values are determined by weak interactions (e.g., the interlayer distance in graphite), the LDA functional is more accurate than the generalized gradient approximation functionals.

DOI: 10.1103/PhysRevB.75.115131 PACS number(s): 71.15.Mb, 31.15.Ew, 68.35.−p, 34.30.+h

I. INTRODUCTION

The Kohn-Sham[1] version of density functional theory[2] (DFT) is the most used quantum-mechanical method for studying the geometry and electronic structure of finite (atoms and molecules) and infinite (surfaces and solids) systems. Compared to the *ab initio* post-Hartree-Fock methods [e.g., MP2 and CCSD(T) (Ref. 3)], also widely used in chemistry, the Kohn-Sham method is much faster and thus allows calculations on large systems (up to several thousands of atoms with a linear scaling algorithm[4]). In practical calculations, only approximate functionals for the exchange-correlation energy can be used, and until now, no functional has been proposed that is able to yield reliable results in any circumstance. For molecular systems, hybrid functionals[5,6] are often the most accurate, while for solids, the functionals of the local-density approximation (LDA) and generalized gradient approximation (GGA) are still the most widely used. Note that the last years have seen the emergence of meta-GGA [e.g., PKZB (Refs. 7 and 8) and TPSS (Refs. 9–11)] functionals (both for finite and infinite systems) and the use of hybrid functionals for solids, which, depending on the type of system, work quite successfully (see Ref. 12 for a review). Nevertheless, only very few codes offer the possibility to perform meta-GGA or hybrid calculations for solids. In addition, hybrid calculations remain very expensive for infinite systems due to the slow convergence of the Hartree-Fock energy, unless a screened Coulomb operator is used for the Hartree-Fock energy calculation.[13–15]

Recently, Wu and Cohen[16] (WC) proposed a new GGA exchange-energy functional. Their functional, used in combination with the PBE correlation-energy functional,[17] was shown to have significant improvement over LDA, PBE, and TPSS for the geometrical parameters and the bulk modulus of solids. They also showed that their functional performs as good as PBE for the cohesive energy of solids and as good as TPSS for the jellium surface energy, while it is rather bad at reproducing the exact (Hartree-Fock) exchange energy of rare-gas atoms. The WC functional has interesting features, mainly because it is a GGA functional, which is both easy to implement and computationally efficient and does not contain any adjustable parameter. Therefore, it is of great interest to test its quality for various systems. The WC functional is potentially very interesting, in particular, for surfaces and solids for which the GGA PBE functional (proposed in 1996 by Perdew *et al.*[17]) is still the standard one. Nevertheless, we expect the WC functional to perform similarly as other LDA and GGA functionals concerning the electronic properties of most systems, and no real improvement is expected for systems which are known as difficult cases for LDA and GGA, in particular, those systems where the self-interaction error contained in LDA and GGA is important, e.g., the hydrogen atom and solids containing strongly correlated electrons for which a treatment with the more advanced empirical LDA $+U$ (Ref. 18) or hybrid functionals[12,19] (which lie beyond the Kohn-Sham formalism) is required.

We have chosen a testing set of 76 solids that is larger than the one used by Wu and Cohen.[16] Surfaces were also considered; more specifically, the binding energy of a hexagonal boron nitride (h-BN) monolayer on a metallic substrate as well as the corresponding surface formation energy were calculated. For molecules, both covalent and noncovalent interactions were considered, where the latter provide a particular tough test for the (semi)local (LDA, GGA, and meta-GGA) and hybrid functionals. Note that for the treatment of noncovalent interactions within the DFT framework, other strategies or types of functionals were designed. Recent articles include the method based on subsystems,[20] a model

based on the dipole moment of the exchange hole,[21] a fully nonlocal correlation-energy functional,[22] and the explicit inclusion of the dispersion energy.[23] For the present work, we have tested only such functionals that are derived from the homogeneous electron gas and mathematical relations obeyed by the exact functional. We note that such functionals are sometimes called "nonempirical" in the literature (see, e.g., Ref. 24).

The paper is organized as follows. In Sec. II, the tested functionals are briefly presented and the details of the calculations are given. In Sec. III, the results are presented and discussed, and in Sec. IV the conclusions are given.

II. METHOD AND COMPUTATIONAL DETAILS

The exchange-correlation energy E_{xc} is the quantity for which an approximate functional must be chosen for any practical Kohn-Sham calculation. The LDA approximation,[25–27] which is the starting point for the development of most of the other types of approximations, has the following form:

$$E_{xc}^{LDA}[\rho] = \int \varepsilon_{xc}^{LDA}(\rho(\mathbf{r}))d^3r, \tag{1}$$

where $\varepsilon_{xc}^{LDA}(\rho)$ is a function of the electron density ρ (or $\rho_\uparrow$ and $\rho_\downarrow$ for spin-polarized calculations) and can be very accurately calculated in the case of the homogeneous electron gas. In real (inhomogeneous) systems, one can allow for more flexibility by the GGA functionals which also use the first derivative of ρ:

$$E_{xc}^{GGA}[\rho] = \int \varepsilon_{xc}^{GGA}(\rho(\mathbf{r}),|\nabla\rho(\mathbf{r})|)d^3r. \tag{2}$$

For convenience, we give only the exchange part E_x (which represents the largest part of the exchange-correlation energy) of the functionals we tested. We first write the GGA exchange-energy functional in the following form:

$$E_x^{GGA}[\rho] = -C_x \int \rho^{4/3}(\mathbf{r})F(s(\mathbf{r}))d^3r, \tag{3}$$

where $C_x=(3/4)(3/\pi)^{1/3}$ and $F(s)$ is the enhancement factor with $s=|\nabla\rho|/(2\rho k_F)$ and $k_F=(3\pi^2\rho)^{1/3}$. In this notation, the LDA approximation[25] corresponds to $F^{LDA}(s)=1$, which is the exact functional for the homogeneous electron gas. In this work, we used for the LDA correlation energy the VWN5 functional of Vosko *et al.*[26] for finite systems and the PW92 functional of Perdew and Wang[27] for infinite systems. Note that VWN5 and PW92 are both very accurate fits of quantum Monte Carlo results obtained for the homogeneous electron gas.[28] PW91 (Ref. 29) is the oldest of the GGA functionals we considered, and its enhancement factor of the exchange part is

$$F^{PW91}(s) = \frac{1 + 0.196\,45s\,\mathrm{arcsinh}(7.7956s) + (0.2743 - 0.1508e^{-100s^2})s^2}{1 + 0.196\,45s\,\mathrm{arcsinh}(7.7956s) + 0.004s^4}. \tag{4}$$

PW91 was the standard functional for early GGA calculations on solids, but then it was replaced by PBE (Ref. 17) that gives very similar results, but has a much simpler analytical expression for the exchange part, namely,

$$F^{PBE}(s) = 1 + \kappa - \frac{\kappa}{1 + \frac{\mu}{\kappa}s^2}, \tag{5}$$

where $\kappa=0.804$ and $\mu=0.219\,51$. Recently, Wu and Cohen[16] proposed another PBE-like modification for the exchange-energy functional:

$$F^{WC}(s) = 1 + \kappa - \frac{\kappa}{1 + \frac{x}{\kappa}}, \tag{6}$$

where $\kappa=0.804$ and

$$x = \frac{10}{81}s^2 + \left(\mu - \frac{10}{81}\right)s^2e^{-s^2} + \ln(1 + cs^4), \tag{7}$$

where $\mu=0.219\,51$ and $c=0.007\,932\,5$. The form and coefficients of Eqs. (6) and (7) were chosen in order to reproduce the fourth-order gradient expansion of the exact exchange-energy functional in the limit of a slowly varying density.[30] This requirement could reveal more important for solids, where the electron density is more homogeneous than in atoms and molecules. Note that various authors proposed other PBE-like functionals[31–35] and that among them, RPBE, (Ref. 32) was also constructed using only mathematical properties of the exact functional. Nevertheless, we did not consider this functional in our study because it has already been shown that RPBE performs quite badly for the lattice constant and bulk modulus of solids.[8,16,35]

From Fig. 1, we can see that for s smaller than $s\simeq 4$, the enhancement factor of WC is slightly smaller than that of PW91 and PBE, but for larger values of s, PBE and WC factors are very close to each other. The PW91 factor, however, goes to zero after it has reached a maximum at $s\simeq 3.8$. It was noted by Wesolowski *et al.*[36] and Zhang *et al.*[37]

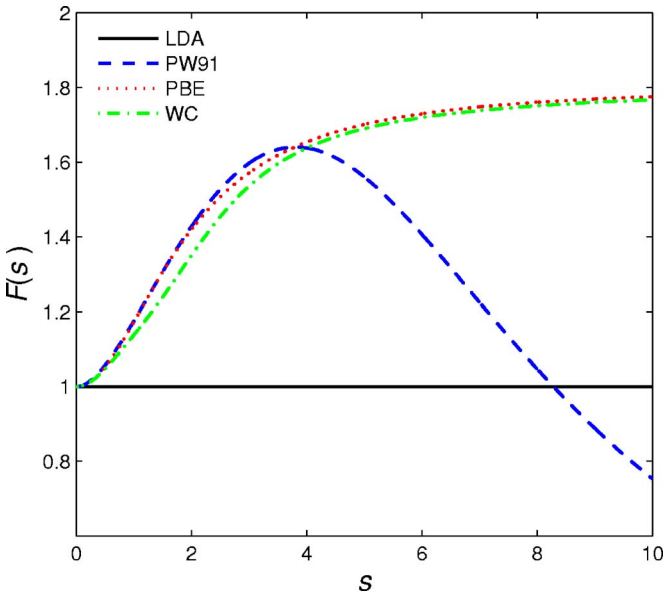

FIG. 1. (Color online) Enhancement factors $F(s)$ of LDA, PW91 [Eq. (4)], PBE [Eq. (5)], and WC [Eq. (6)] exchange-energy functionals.

that for the description of noncovalent interactions, the behavior of the exchange functional in regions of large s (i.e., low-density and large-density gradients) plays an important role.

The molecular calculations of Sec. III A were done with the DEMON code,[38] which uses Gaussian basis sets to solve the Kohn-Sham equations. For most calculations, the large uncontracted basis sets developed by Partridge[39,40] were used. The basis sets and grid integrations are large enough to be confident that our results are very close to the fully converged results, both for the covalent (Sec. III A 1) and noncovalent (Sec. III A 2) systems. The interaction energies of the noncovalently bound complexes of Sec. III A 2 were corrected for the basis-set superposition error (BSSE) by means of the counterpoise correction method of Boys and Bernardi.[41] With the Partridge basis sets, the value of the BSSE is situated in the range 0.05–0.1 kcal/mol for noncovalent systems that are bound by more than 10 kcal/mol, while it is much smaller for very weakly bound systems (for instance, for Ne_2 the BSSE amounts to 0.006 kcal/mol). These small values for the BSSE are a good indication that the Partridge basis sets are close to the complete saturation. Only for the geometry optimization of the charge-transfer complexes was a smaller basis set (triple zeta valence with polarization[42]) used, and no counterpoise correction was used to remove the BSSE.

The periodic calculations (surfaces and solids) of Secs. III B and III C were done with the WIEN2K code,[43] which is based on the full-potential (linearized) augmented plane-wave and local orbitals method to solve the Kohn-Sham equations. The surface calculations were done with a slab geometry. In order to ensure convergence of the formation energies, the thickness of the slab was varied from 7 to 13 layers for fcc metals and from 8 to 14 layers for hcp metals. The thickness of the vacuum region was set to about 13 Å. The formation energies were calculated using slab energies with m and n layers as $(mE_n - nE_m)/(n-m)$.[44] The binding energy and geometry of epitaxially deposited h-BN on transition-metal systems were calculated with seven layer metal slabs. The Brillouin-zone integrations were performed with a $21\times21\times1$ special point grid. For the bulk calculations, the Brillouin-zone integrations were performed with a $21\times21\times21$ grid for most solids. The exceptions are MnO, FeO, CoO, and NiO for which a $18\times18\times18$ grid was used in the rhombohedral Brillouin zone (antiferromagnetic order along the [111] direction), and the layered-systems C (graphite), BN, and $MoSe_2$ for which the integrations were performed with the $14\times14\times4$, $19\times19\times2$, and $20\times20\times4$ grids, respectively. For most calculations, the value of $R_{\mathrm{MT}}^{\mathrm{min}}K_{\mathrm{max}}=10$ (the product of the smallest of the atomic sphere radii R_{MT} and the plane-wave cutoff parameter K_{max}) was used for the expansion of the basis set. In some cases, mainly lighter elements, a smaller value of $R_{\mathrm{MT}}^{\mathrm{min}}K_{\mathrm{max}}$ was used (8–9) in order to avoid problems with linear dependencies. Spin-orbit coupling was taken into account for the solids containing Ba, La, Ce, Hf, Ta, W, Ir, Pt, Au, and Th atoms.

The chosen parameters of convergence for both the molecular and periodic calculations are by far sufficient for testing the functionals, which is the main purpose of the present work. For the analysis of the calculations, the following statistical quantities will be used: the mean error (me), the mean absolute error (mae), the mean relative error (mre, in%), and the mean absolute relative error (mare, in%).

III. RESULTS

A. Molecules

1. Covalent bonds

In Table I, displayed are the results for the bond length and atomization energy of 19 small covalent molecules. This set of molecules is the same as the one chosen in Refs. 7, 8, and 17, but without Be_2, since this metal dimer is bound by noncovalent interactions. The results show that for the bond length, the performances of PBE and WC are similar, with the me and mae just below 0.01 Å. Like PBE, WC has the tendency to overestimate the bond lengths (me=0.006 Å), which is not the case with LDA (me=0.001 Å), with this set of molecules. For most molecules, WC gives a bond length situated between LDA and PBE bond lengths (closer to PBE), which is not too surprising if we recall that the WC enhancement factor $F(s)$ is below the PBE enhancement factor (Fig. 1) for the small s region. For H_2, LiH, and Li_2 molecules, in particular, WC yields bond lengths that are larger than PBE bond lengths.

The WC functional gives worse atomization energies than PBE (12.6 and 8.1 kcal/mol for the mae, respectively), where the latter is already a rather poor functional compared to the best (but containing many adjustable parameters) GGA and hybrid functionals, which have an accuracy of 2–3 kcal/mol (see Refs. 10 and 45 for recent extensive tests). WC yields atomization energies that, similar to its bond lengths, are situated between the LDA and PBE values for all molecules except H_2, LiH, and Li_2. These three mol-

TABLE I. Equilibrium bond length R_0 (Å) and atomization energy ΔE (kcal/mol) of 19 covalent molecules.

	R_0				ΔE			
Molecule	LDA	PBE	WC	Expt.	LDA	PBE	WC	Expt.
H_2	0.764	0.749	0.754	0.741	113.5	104.8	104.2	109.5
LiH	1.601	1.602	1.605	1.595	67.7	60.1	59.4	57.8
CH_4	1.096	1.095	1.094	1.087	462.7	420.3	426.3	419.3
NH_3	1.021	1.020	1.020	1.012	338.1	302.8	307.1	297.4
OH	0.984	0.981	0.981	0.970	124.5	110.4	112.5	106.4
H_2O	0.969	0.968	0.967	0.957	267.3	235.4	240.9	232.2
HF	0.931	0.930	0.929	0.917	162.5	142.6	146.6	140.8
Li_2	2.649	2.670	2.682	2.673	31.0	27.3	26.8	24.4
LiF	1.548	1.573	1.564	1.564	163.7	146.3	149.1	138.9
C_2H_2 (CC)	1.201	1.207	1.205	1.202	458.8	413.9	422.0	405.4
C_2H_2 (CH)	1.074	1.070	1.071	1.063				
C_2H_4 (CC)	1.323	1.333	1.329	1.339	632.6	571.7	582.1	562.6
C_2H_4 (CH)	1.093	1.090	1.090	1.087				
HCN (HC)	1.079	1.075	1.076	1.066	359.6	325.2	330.6	311.9
HCN (CN)	1.150	1.158	1.155	1.153				
CO	1.127	1.136	1.132	1.128	298.1	268.5	274.8	259.3
N_2	1.095	1.103	1.100	1.098	266.1	242.5	245.1	228.5
NO	1.146	1.157	1.153	1.151	197.8	171.6	176.4	152.9
O_2	1.204	1.219	1.213	1.208	174.1	143.5	150.9	120.5
F_2	1.388	1.417	1.405	1.412	77.4	52.7	59.0	38.5
P_2	1.894	1.908	1.902	1.893	141.9	120.3	125.6	117.3
Cl_2	1.994	2.018	2.005	1.988	82.5	66.0	71.4	58.0
me	0.001	0.008	0.006		33.6	7.6	12.1	
mae	0.010	0.009	0.007		33.6	8.1	12.6	
mre	0.29	0.66	0.51		23.6	6.7	9.7	
mare	0.85	0.71	0.62		23.6	7.2	10.2	

ecules have relatively weak covalent bonds, and it will be shown below, in Sec. III A 2, that the same behavior occurs for noncovalent complexes bound by very weak van der Waals interactions.

2. Noncovalent bonds

In this section, the performances of LDA, PW91, PBE, and WC functionals on noncovalent interactions are assessed. To this end, the five benchmark databases recently proposed by Zhao and Truhlar[46,47] were chosen. These databases (see Table II) consist of reference interaction energies ΔE of six hydrogen bonding complexes (HB6), seven charge-transfer complexes (CT7), six dipole interaction complexes (DI6), seven weak interaction complexes (WI7), and five π-π stacking interaction complexes (PPS5). These reference interaction energies were determined from experimental studies for C_6H_6-Ne (Ref. 48) and the rare-gas dimers[49,50] and extrapolation at the basis set limit of CCSD(T) calculations for the benzene dimer[51] and the other complexes[46,52] (see Ref. 46 for details). We note that Zhao and Truhlar[46] did not test the PW91 functional, which can be considered obsolete since PBE (which yields very similar results in most cases) was proposed. Nevertheless, for noncovalent interactions, PW91 and PBE can lead to qualitatively different results (see also Ref. 53 for differences in monovacancy formation energies) and PW91 has sometimes been considered a good functional for noncovalent interactions (see, e.g., Refs. 54 and 55). The interaction energies of Table II were calculated at an *ab initio*-determined geometry [CCSD(T) for the three geometries of the benzene dimer[56] and MC-QCISD/3 (Ref. 46) for the other complexes]. This procedure for calculating ΔE without DFT-geometry optimization can be considered a good one for most functionals and complexes.[46] Nevertheless, due to the usual strong underestimation of the intermolecular distance by LDA, the LDA interaction energy is expected to show a non-negligible increase if a LDA geometry optimization is performed.[46] The same trend was observed with other functionals (in particular PBE) for charge-transfer complexes,[46] and this is the reason why we did a geometry optimization for them (Table IV). We also considered the geometry optimization of the rare-gas dimers (Table V), which represent the archetypical class of intensively studied pure van der Waals complexes,[37,57–61] for

TABLE II. Counterpoise-corrected interaction energy ΔE (kcal/mol) of five types of noncovalent complexes (proposed benchmark databases) calculated at the *ab initio*-determined geometry (see text). A negative value indicates a nonstable complex.

Complex	LDA	PW91	PBE	WC	Reference
		HB6			
$(NH_3)_2$	5.19	3.37	3.13	3.34	3.15
$(HF)_2$	7.11	4.93	4.66	4.91	4.57
$(H_2O)_2$	7.75	5.28	5.00	5.39	4.97
NH_3-H_2O	10.04	7.17	6.87	7.49	6.41
$(HCONH_2)_2$	21.62	15.27	14.75	16.34	14.94
$(HCOOH)_2$	26.08	18.49	17.83	20.16	16.15
		CT7			
C_2H_4-F_2	4.58	3.18	2.90	2.81	1.06
NH_3-F_2	7.58	5.43	5.18	5.25	1.81
C_2H_2-ClF	10.48	6.42	6.07	7.11	3.81
HCN-ClF	9.82	6.01	5.68	6.48	4.86
NH_3-Cl_2	12.21	8.36	8.06	9.05	4.88
H_2O-ClF	11.42	7.46	7.12	8.00	5.36
NH_3-ClF	25.31	18.31	17.85	20.28	10.62
		DI6			
$(H_2S)_2$	3.38	1.89	1.70	1.85	1.66
$(HCl)_2$	3.87	2.20	1.99	2.16	2.01
HCl-H_2S	6.58	4.28	4.05	4.51	3.35
CH_3Cl-HCl	6.39	3.50	3.22	3.68	3.55
HCN-CH_3SH	5.84	3.76	3.48	3.77	3.59
CH_3SH-HCl	9.23	5.79	5.49	6.29	4.16
		WI7			
He-Ne	0.15	0.26	0.09	0.06	0.04
He-Ar	0.17	0.26	0.09	0.05	0.06
Ne_2	0.26	0.33	0.13	0.07	0.08
Ne-Ar	0.33	0.34	0.14	0.06	0.13
CH_4-Ne	0.38	0.37	0.15	0.06	0.22
C_6H_6-Ne	0.87	0.40	0.11	−0.06	0.47
$(CH_4)_2$	0.95	0.25	0.02	−0.15	0.51
		PPS5			
$(C_2H_2)_2$	2.08	1.17	0.96	0.88	1.34
$(C_2H_4)_2$	2.49	0.57	0.33	0.23	1.42
$(C_6H_6)_2$-S	0.84	−0.96	−1.25	−1.56	1.81
$(C_6H_6)_2$-T	2.96	0.72	0.43	0.55	2.74
$(C_6H_6)_2$-PD	2.12	−0.54	−0.85	−0.95	2.78

which only dispersion forces contribute to the interaction.

From the results of Tables II and III, we can see that the trend is the same among the three different databases HB6, CT7, and DI6. Compared to the reference results, all four functionals show a clear trend to overestimate (i.e., to overbind) ΔE for most complexes. From the smallest overestimation to the largest, the order of the functionals is PBE, PW91, WC, and LDA. Concerning the WI complexes, LDA overestimates the interaction energy ΔE for all complexes. PW91 and PBE also overestimate ΔE for the rare-gas dimers, while the interaction energy of CH_4-Ne is underestimated by PBE and that of C_6H_6-Ne by PW91 and PBE. Somewhat surprisingly, WC is the functional which yields the smallest interaction energies. It gives values for ΔE which are quasi-identical to the reference values for He-Ne, He-Ar, and Ne_2 complexes and underestimates ΔE for the other complexes of the WI7 database. We recall that in Sec. III A 1, WC was the functional with the smallest atomization energies for H_2, LiH, and Li_2 molecules. The results for the PPS5 database clearly show that LDA is the best functional.

TABLE III. Statistics on the interaction energies of Table II. See the text for the definition of the quantities.

	LDA	PW91	PBE	WC
		HB6		
me	4.60	0.72	0.34	1.24
mae	4.60	0.72	0.41	1.24
mre	56	8	3	12
mare	56	8	4	12
		CT7		
me	7.00	3.25	2.92	3.80
mae	7.00	3.25	2.92	3.80
mre	190	96	86	100
mare	190	96	86	100
		DI6		
me	2.83	0.52	0.27	0.66
mae	2.83	0.53	0.42	0.66
mre	93	16	7	19
mare	93	16	11	19
		WI7		
me	0.23	0.10	−0.11	−0.20
mae	0.23	0.19	0.15	0.21
mre	153	191	5	−48
mare	153	210	64	64
		PPS5		
me	0.08	−1.83	−2.09	−2.19
mae	0.73	1.83	2.09	2.19
mre	12	−84	−98	−104
mare	43	84	98	104
		All		
me	3.08	0.70	0.41	0.83
mae	3.19	1.32	1.19	1.62
mre	108	56	7	1
mare	113	87	53	60

The mae of LDA is 0.73 kcal/mol, and the me of 0.08 kcal/mol indicates that LDA does not systematically underestimate or overestimate the interaction energy of PPS interaction complexes. The GGA functionals underestimate ΔE for all complexes of the PPS5 database. The interaction energies of $(C_2H_4)_2$ and the benzene dimer in the T-shaped (T) geometry are strongly underestimated, while the sandwich (S) and parallel-displaced (PD) geometries of the benzene dimer are even unstable (at the *ab initio* intermolecular distances) with GGA.

Among the numerous DFT functionals tested by Zhao and Truhlar,[46,47] PBE was shown to be a very good one for the HB, DI, and WI complexes (see also Ref. 62 for HB complexes). For the CT interactions, all four tested functionals perform very badly with me and mae of 7.00, 3.25, 2.92, and 3.80 kcal/mol for LDA, PW91, PBE, and WC, respectively. These values for the mae are much larger than what is obtained with the best performing functionals (~0.2–0.5 kcal/mol with several hybrid and meta-GGA-hybrid functionals).[46,47] LDA performs very well for PPS interaction complexes, like it does for graphite solid (see, e.g., Refs. 23 and 63).

Depending on the DFT functional, a very large increase of the interaction energy for the CT complexes, with respect to the one calculated at the MC-QCISD/3 geometry, can be obtained if a geometry optimization is also performed with the considered DFT functional.[46] Therefore, we also performed a DFT-geometry optimization of the CT complexes (with the TZVP basis set[42] and without the counterpoise correction) for the calculation of ΔE. Indeed, our results, displayed in Table IV, show that a dramatic increase of ΔE is obtained with all four functionals. Now, the interaction energies are overestimated by 11.88, 6.22, 5.79, and 7.15 kcal/mol with LDA, PW91, PBE, and WC, respectively, which represents several hundred percent for the mare. In contrast, the best hybrid functionals lead to small mae of less than 0.5 kcal/mol with a geometry optimization.[46]

A geometry optimization was also performed for the van der Waals rare-gas dimers (results in Table V). The results are compared to the experimental bond lengths and interaction energies of Refs. 49 and 50. It is well known that LDA underestimates the intermolecular bond length R_0, and for the rare-gas dimers, the underestimation is particularly high (0.3–0.5 Å). This leads to a strong overestimation of ΔE (0.34 kcal/mol, 371%). PW91 underestimates (overestimates) R_0 of the lightest (heaviest) dimers and gives the best results for the intermediate dimers Ne-Ar and Ne-Kr. Despite the significant improvement of PW91 over LDA for bond lengths, it still significantly overestimates the interaction energy of most dimers. The PBE bond lengths are ~0.1 Å larger than the PW91 values, and with respect to PBE, the WC functional systematically increases R_0 by ~0.2 Å, which means an overestimation of R_0 for all dimers except He_2 (which has an underestimation of 0.05 Å). WC shows a clear trend to underestimate ΔE for most dimers (−0.078 kcal/mol for the me). Among the four tested functionals, PBE is the most accurate for the bond length and interaction energy if the mae is considered (0.15 Å and 0.077 kcal/mol), and for the mare, PBE remains the best for R_0 (4.1%), while WC slightly improves over PBE for ΔE with 48%. In Fig. 2, we show the LDA, PW91, PBE, and WC interaction energy curves of Ne_2 and Ar_2 dimers and compare them with the reference values (represented by ×). For Ne_2, PBE yields the exact value for R_0, while WC gives a very good interaction energy. For Ar_2, PW91 is the best functional overall. Note that very recently, Zhao and Truhlar[61] tested 18 functionals (LDA, GGA, meta-GGA, hybrid, and meta-GGA-hybrid) on this same set of rare-gas dimers, and PBE was shown to be one of the most accurate functionals.

B. Surfaces

In order to test the performance of the functionals on surfaces, we have chosen a set of 3*d*, 4*d*, and 5*d* transition-

TABLE IV. Interaction energy ΔE (kcal/mol) of the complexes of the CT7 database calculated after geometry optimization. The TZVP basis set was used and the results were not corrected for the BSSE.

Complex	LDA	PW91	PBE	WC	Reference
C_2H_4-F_2	17.04	11.57	11.05	11.91	1.06
NH_3-F_2	19.64	14.23	13.67	14.56	1.81
C_2H_2-ClF	13.12	7.46	7.11	8.72	3.81
HCN-ClF	12.61	6.91	6.51	7.90	4.86
NH_3-Cl_2	15.77	10.09	9.68	11.33	4.88
H_2O-ClF	13.38	8.37	8.06	9.12	5.36
NH_3-ClF	23.99	17.31	16.88	18.92	10.62
me	11.88	6.22	5.79	7.15	
mae	11.88	6.22	5.79	7.15	
mre	485	292	275	314	
mare	485	292	275	314	

metal surfaces. Because such metal surfaces attracted a lot of attention as a substrate for molecular deposition, we also tested the behavior of the functionals on the binding of a h-BN layer to these metal surfaces.[64]

In Table VI, we list the calculated surface formation energies for a set of ten metals. The surfaces considered are (111) for fcc metals (Ni, Cu, Rh, Pd, Ag, Ir, Pt, and Au), and (0001) for hcp metals (Co and Ru). The metal surface formation energies are rather well studied quantities within DFT methods.[44,65] Our LDA and PBE results are close to the results of previous studies.[44,65] As we can see, for all metals, the LDA shows the highest and PBE the lowest calculated formation energies, while the WC functional always gives values in between. For the 3*d* metals (Co, Ni, and Cu) the LDA and PBE functionals yield too large and too small values, respectively, with respect to the measured values.[66,67] The WC results compare very well with experiment for Co and Ni. For 4*d* elements (Ru, Rh, Pd, and Ag), the LDA functional is definitely the best one, while WC slightly underestimates and PBE severely underestimates the surface energies. For the lighter Ru and Rh, the WC functional produces results with an error around 10%, while for the heavier elements, the error exceeds 15%. For 5*d* elements (Ir, Pt, and Au), the differences between the calculations and experiments are even larger. For Ir, LDA slightly overestimates the surface formation energy, while WC and, in particular, PBE underestimate it. For Pt and Au, all three functionals strongly underestimate the surface formation energy, probably because the experimentally observed surface reconstructions have been neglected. Overall, the LDA functional leads to the smallest values for the me and mae, closely followed by WC, while PBE is significantly less accurate.

The binding energies and geometries of a h-BN layer on top of metal surfaces are presented in Table VII. While for Ni and Cu the lattice mismatch is small and thus epitaxial monolayers of h-BN were also found experimentally,[68] on systems with a larger lattice mismatch, more complicated moiré pattern[69] or even highly complex nanostructures (Ru, Rh) were found.[70] We neglected the more complicated structures but strained BN as required to be able to place it epitaxially at the (fcc, top) position above the metal, which was found to be the most favorable adsorption site in all cases. Like in the case of the surface formation energies, for all metals, the LDA and PBE functionals produce the largest and smallest binding energies, respectively, whereas the WC functional gives values in between. For the three cases, Cu, Ag, and Au, the PBE functional does not show any binding (i.e., negative ΔE), which at least in the case of Cu is clearly in contradiction with experiment where such a layer is observed, although it is not as stable as the Ni system.[71] Considering the stability of the observed h-BN monolayers on Ni, Cu, Rh, Pd, and Pt,[68–72] it can be concluded that PBE gives too small binding energies and LDA seems to overestimate them. In all these cases, the WC functional seems to improve the theoretical results. The h-BN layer is no longer flat but slightly buckled with the B atom closer to the metal than the N atom in all cases. This buckling (vertical B-N distance z_{B-N}), as well as the vertical metal-N distance z_{M-N}, follows the trend seen in the binding energies and is smallest with LDA but largest for PBE (Table VII).

C. Solids

For the testing of the functionals on solids, we chose a set of 76 solids (see Tables VIII and IX), including magnetic and nonmagnetic metals, semiconductors, and insulators. Experimental data for the equilibrium lattice constant a_0 and bulk modulus B_0 are available in the literature.[11,14,73–105] Among them, there are the layered-systems graphite, h-BN, and $MoSe_2$, whose distances between the layers are determined by rather weak interactions. Our set also includes the rare-gas solids that are stabilized by pure van der Waals interactions.

Considering first the elemental solids, we can see that LDA strongly underestimates the lattice constant by 0.1–0.3 Å for groups I (Li, Na, K, and Rb) and II (Ca, Sr, and Ba). PBE and WC functionals partially correct the failure of LDA, with WC being the best for group I and PBE for group II (but still with a clear underestimation for Ca and Sr). For Al (group III), there is also a strong underestimation of a_0 by LDA, while the PBE value is very close to the experimental one. Concerning group IV, namely, C (in the

TABLE V. Counterpoise-corrected equilibrium bond length R_0 (Å) and interaction energy ΔE (kcal/mol) of ten rare-gas dimers.

	R_0					ΔE				
Complex	LDA	PW91	PBE	WC	Expt.[a]	LDA	PW91	PBE	WC	Expt.[a]
He_2	2.43	2.65	2.78	2.92	2.97	0.186	0.246	0.074	0.054	0.022
Ne_2	2.64	3.01	3.08	3.25	3.09	0.463	0.333	0.129	0.081	0.084
Ar_2	3.41	3.96	4.02	4.27	3.76	0.699	0.343	0.159	0.100	0.285
Kr_2	3.71	4.32	4.37	4.63	4.01	0.804	0.356	0.174	0.111	0.400
He-Ne	2.49	2.82	2.91	3.07	3.03	0.328	0.286	0.097	0.063	0.041
He-Ar	2.96	3.34	3.45	3.63	3.48	0.308	0.268	0.087	0.057	0.057
He-Kr	3.15	3.53	3.66	3.83	3.69	0.294	0.259	0.086	0.056	0.057
Ne-Ar	3.03	3.47	3.54	3.75	3.49	0.545	0.337	0.139	0.086	0.134
Ne-Kr	3.19	3.65	3.72	3.93	3.62	0.564	0.343	0.144	0.090	0.142
Ar-Kr	3.56	4.14	4.20	4.45	3.88	0.745	0.349	0.165	0.105	0.361
me	−0.44	−0.01	0.07	0.27		0.335	0.154	−0.033	−0.078	
mae	0.44	0.17	0.15	0.28		0.335	0.165	0.077	0.089	
mre	−13.0	−0.9	1.6	7.3		371	294	38	−9	
mare	13.0	5.0	4.1	7.6		371	296	69	48	

[a]References 49 and 50.

diamond and graphite structures), Si, Ge, and Sn, the WC functional is better for C and Si, while LDA is better for the heavier elements Ge and Sn. PBE overestimates a_0 for most group-IV elements. For the 3*d* transition metals we considered (V, Fe, Ni, and Cu), PBE is clearly the best functional, while LDA and WC systematically underestimate the lattice constant. Concerning the case of the 4*d* transition metals (Nb, Mo, Rh, Pd, and Ag), WC is the functional yielding values for a_0, which are closest to the experimental ones, while with LDA and PBE, there is underestimation and overestimation, respectively. For the heavier 5*d* metals (Ta, W, Ir, Pt, and Au), PBE also overestimates the lattice constants. The WC functional is better for the two lightest of these 5*d* transition metals, while for the heavier, LDA is the most accurate functional. All three functionals give lattice constants which are smaller than the experimental one for the actinide Th. From Table IX, we can see that all three functionals perform badly for the rare-gas solids. LDA underestimates a_0 by 0.3–0.6 Å, while with PBE there is an overestimation of at least 0.7 Å for all rare gases except Ne, and WC increases a_0 further by 0.3–0.5 Å with respect to PBE. This behavior was expected according to the results of Table V on rare-gas dimers.

Turning now to the *AB* compounds, trends among the different types can also be observed. For the group-I-VII ionic compounds (LiF, LiCl, NaF, and NaCl), we can clearly see that LDA underestimates and PBE overestimates the lattice constant, while WC values are in between and in much better agreement with the experimental values. For the transition-metal carbides and nitrides (TiC, VC, ZrC, NbC, HfC, ScN, TiN, VN, YN, ZrN, NbN, and HfN), PBE lattice constants are very accurate if the metal belongs to the 3*d* row, while for the 4*d* and 5*d* metals, WC performs better. For the group-II-VI compounds, WC performs better than LDA and PBE for MgO and MgS, while PBE is slightly better for CaO. Concerning the transition-metal oxides (MnO, FeO, CoO, NiO, and ZnO), LDA gives by far too small lattice constants and the WC functional is not really able to repair the failure of LDA. Overall, the PBE functional is much better for these compounds. Note that with both LDA and GGA, FeO and CoO are incorrectly described as being metallic instead of insulators, a fact which can have some influ-

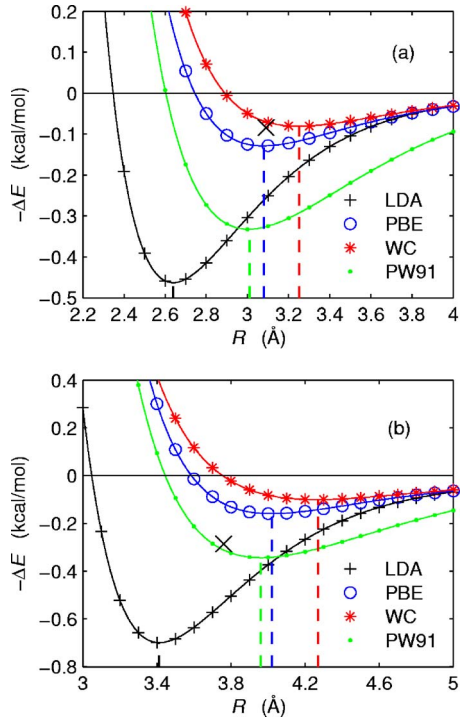

FIG. 2. (Color online) Ne_2 (a) and Ar_2 (b) interaction energy curves. The reference results (Ref. 49) are indicated by a black cross.

TABLE VI. Surface formation energy. For each functional, values in eV/atom (left column) and J/m^2 (right column) are given. Both sets of experimental values are in J/m^2. The me and mae were calculated with respect to the average of the two sets of experimental values.

	LDA		PBE		WC		Expt.[a]	
Co	0.89	2.82	0.73	2.17	0.83	2.54	2.52	2.55
Ni	0.81	2.55	0.66	1.98	0.75	2.32	2.38	2.45
Cu	0.62	1.87	0.48	1.36	0.57	1.65	1.79	1.83
Ru	1.22	3.11	1.06	2.62	1.17	2.95	3.04	3.05
Rh	1.00	2.63	0.80	2.03	0.94	2.41	2.66	2.70
Pd	0.77	1.94	0.59	1.40	0.70	1.72	2.00	2.05
Ag	0.53	1.23	0.36	0.78	0.46	1.04	1.25	1.25
Ir	1.26	3.20	0.88	2.16	1.05	2.63	3.05	3.00
Pt	0.84	2.06	0.65	1.52	0.75	1.79	2.49	2.48
Au	0.44	1.00	0.28	0.59	0.38	0.84	1.51	1.50
me		−0.04		−0.62		−0.29		
mae		0.18		0.62		0.29		

[a]References 66 and 67 for the left and right columns, respectively.

ence on the structure. The situation is similar to that of the intermetallic compounds FeAl, CoAl, and NiAl, in which PBE gives relatively accurate lattice constants, whereas LDA and WC values are systematically too small. For the III-V semiconductors (AB, where A=B, Al, Ga, In and B=N, P, As), WC is clearly the best functional, while there is a systematic underestimation and overestimation with LDA and PBE, respectively. For SiC and CeO_2, the WC functional is very accurate. Special attention is paid to layered compounds such as graphite [C (A9)], h-BN (B_k), and $MoSe_2$. While the in-plane lattice parameter a_0 is most accurate with WC, but PBE and even LDA are not that much off either, the situation is completely different for the c_0 parameter. As can be seen in Fig. 3, only LDA gives well defined minima and reasonable binding energy curves with a stabilization of the bulk vs the monolayer of about 8 mRy per unit cell. Both GGAs show only marginal binding of the hexagonal layers along c, although the left-hand side (small c) of the potential-energy curves looks as expected, with PBE clearly too large and WC and LDA close to experiment.

The statistics on the set of lattice constants of Table VIII shows that the WC functional is the best among the three tested functionals with, e.g., 0.031 Å for the mae and 0.7% for the mare. LDA is only in six cases the best functional, PBE in 31, and WC leads in 43 cases to the best values. For the lattice constants related to weak interactions (Table IX), LDA is the functional which leads to the smallest statistical errors. Note that the meta-GGA functional TPSS (Refs. 9–11) yields, most of the time, a lattice constant which is smaller than the PBE value by 0.01–0.02 Å, resulting in slightly smaller mean errors.[11,13,14] Exceptions are the alkali metals Li, Na, and K, for which the TPSS values are larger than the PBE values (also observed with the WC functional for Li and Na, but to a lesser extent).

TABLE VII. Binding energies ΔE (eV/BN) and geometries (Å) of h-BN/transition-metal systems: vertical metal (M)-N ($z_{M\text{-N}}$) and vertical B-N ($z_{\text{B-N}}$) distances. A negative value for ΔE indicates an unbound system. In all cases, the B atom is closer than the N atom to the metal surface.

	LDA			PBE			WC		
	ΔE	$z_{M\text{-N}}$	$z_{\text{B-N}}$	ΔE	$z_{M\text{-N}}$	$z_{\text{B-N}}$	ΔE	$z_{M\text{-N}}$	$z_{\text{B-N}}$
Co	0.32	2.14	0.11	0.06	2.14	0.12	0.23	2.15	0.12
Ni	0.27	2.12	0.11	0.04	2.15	0.11	0.19	2.14	0.11
Cu	0.19	3.10	0.02	−0.01			0.05	3.00	0.01
Ru	0.98	2.13	0.14	0.64	2.18	0.15	0.85	2.17	0.15
Rh	0.61	2.16	0.13	0.31	2.20	0.14	0.50	2.18	0.14
Pd	0.47	2.21	0.11	0.20	2.25	0.12	0.36	2.25	0.12
Ag	0.19	2.55	0.04	−0.01			0.10	2.78	0.03
Ir	0.49	2.20	0.14	0.20	2.24	0.15	0.38	2.23	0.15
Pt	0.34	2.26	0.12	0.05	2.31	0.13	0.19	2.30	0.13
Au	0.16	2.95	0.02	−0.03			0.07	2.93	0.03

TABLE VIII. Equilibrium lattice constant a_0 (Å) and bulk modulus B_0 (GPa) of 72 solids. The Strukturbericht symbols (in parentheses) are used for the structure as follows: A1, fcc; A2, bcc; A4, diamond; B1, rocksalt; B2, cesiumchloride; B3, zinc blende; C1, fluorite; and A9, B_k, and C7, hexagonal structures. The statistics for B_0 does not include solids for which a range or no value is given for experiment. Fe and Ni are ferromagnetic and MnO, FeO, CoO, and NiO are antiferromagnetic (the order is along the [111] direction). Spin-orbit coupling was taken into account for the solids containing Ba, La, Ce, Hf, Ta, W, Ir, Pt, Au, and Th atoms. The best theoretical values are in boldface and the "very bad" results are in italics (with an absolute relative error larger than 2.5% and 30% for a_0 and B_0, respectively).

	a_0				B_0			
Solid	LDA	PBE	WC	Expt.[a]	LDA	PBE	WC	Expt.[a]
Li (A2)	*3.363*	3.435	**3.449**	3.477	15.2	14.0	**13.4**	13.0
C (A4)	3.536	**3.575**	**3.558**	3.567	469	**434**	**451**	443
C (A9)	2.447	2.471	**2.460**	2.464				
Na (A2)	*4.047*	**4.196**	**4.199**	4.225	9.41	7.85	**7.32**	7.5
Al (A1)	3.983	**4.041**	4.023	4.047	84.3	**79.2**	80.6	73
Si (A4)	5.407	5.475	**5.437**	5.430	**96.4**	88.7	94.0	99.2
K (A2)	*5.045*	5.282	**5.256**	5.225	4.50	**3.61**	3.49	3.7
Ca (A1)	*5.333*	**5.530**	5.458	5.58	18.7	**17.3**	**17.4**	15
V (A2)	*2.932*	**3.001**	2.965	3.03	*213*	**183**	198	162
Fe (A2)	*2.753*	**2.830**	*2.791*	2.868	*256*	**194**	*227*	167
Ni (A1)	*3.423*	**3.518**	3.468	3.524	*259*	**200**	231	184
Cu (A1)	*3.522*	**3.632**	3.573	3.615	*191*	**141**	168	133
Ge (A4)	**5.632**	5.769	5.686	5.652	**72.7**	59.5	67.8	75.8
Rb (A2)	*5.374*	5.670	**5.609**	5.59	3.59	**2.77**	2.71	3.06
Sr (A1)	*5.786*	**6.027**	*5.914*	6.08	14.4	11.4	**12.2**	12
Nb (A2)	3.250	**3.312**	3.280	3.30	193	**171**	183	170
Mo (A2)	3.116	**3.164**	**3.139**	3.15	294	260	**279**	272
Rh (A1)	3.759	3.834	**3.795**	3.798	320	**259**	292	269
Pd (A1)	3.848	3.948	**3.892**	3.881	231	170	**207**	195
Ag (A1)	4.007	4.152	**4.065**	4.069	*140.4*	91.0	**118.9**	109
Sn (A4)	**6.481**	*6.661*	6.548	6.481	**45.7**	*36.3*	42.4	53
Ba (A2)	*4.753*	**5.024**	*4.871*	5.02	**10.14**	8.66	9.16	10
Ta (A2)	3.260	3.328	**3.294**	3.304	210	**191**	201	194
W (A2)	3.147	3.196	**3.172**	3.166	323	**290**	307	296
Ir (A1)	**3.834**	3.895	3.864	3.84	385	328	**361**	355
Pt (A1)	**3.923**	3.999	3.958	3.923	**291**	234	**262**	277
Au (A1)	**4.066**	*4.180*	4.113	4.079	187	131	**164**	167
Th (A1)	*4.922*	**5.059**	4.978	5.084	67.1	**59.0**	68.4	58
LiF (B1)	3.919	4.071	**4.017**	4.010	88.2	**67.5**	**72.4**	69.8
LiCl (B1)	4.986	5.167	**5.087**	5.106	42.0	32.2	**35.7**	35.4
NaF (B1)	4.507	4.709	**4.652**	4.609	61.7	44.5	**45.4**	51.4
NaCl (B1)	5.484	5.714	**5.637**	5.595	32.7	23.7	**24.7**	26.6
TiC (B1)	4.266	**4.339**	4.303	4.33	283	**248**	267	233
VC (B1)	4.095	**4.162**	4.129	4.160	349	**307**	328	303
ZrC (B1)	4.647	**4.715**	**4.680**	4.696	**248**	222	236	265
NbC (B1)	4.432	4.491	**4.462**	4.47	335	301	**319**	315
HfC (B1)	4.578	**4.660**	**4.618**	4.638	257	218	238	
ScN (B1)	4.433	**4.518**	4.474	4.50	229	199	213	
TiN (B1)	4.178	**4.254**	4.214	4.239	322	**277**	**300**	288
VN (B1)	4.050	**4.125**	4.087	4.141	*365*	***312***	*340*	233

TABLE VIII. (*Continued.*)

	a_0				B_0			
Solid	LDA	PBE	WC	Expt.[a]	LDA	PBE	WC	Expt.[a]
YN (B1)	4.825	4.912	**4.865**	4.877	183	159	172	
ZrN (B1)	4.532	**4.602**	**4.565**	4.585	*286*	**250**	270	215
NbN (B1)	4.364	4.429	**4.395**	4.392	355	**311**	334	292
LaN (B1)	5.231	**5.324**	**5.270**	5.295	140	123	133	
HfN (B1)	4.482	4.560	**4.520**	4.52	**309**	265	289	306
MgO (B1)	4.169	4.261	**4.223**	4.207	**174**	149	**158**	165
CaO (B1)	4.719	**4.841**	4.777	4.811	129	**105**	**116**	110
MgS (B1)	5.139	5.238	**5.195**	5.20	84.0	74.4	**78.2**	78.9
MnO (B1)	*4.314*	**4.447**	4.382	4.445	183	**148**	166	151
FeO (B1)	*4.178*	**4.301**	4.238	4.334	228	**180**	206	150–180
CoO (B1)	*4.107*	**4.237**	4.167	4.254	*248*	**173**	221	180
NiO (B1)	*4.069*	**4.201**	4.132	4.171	256	**197**	225	166–208
ZnO (B1)	4.221	4.336	**4.273**	4.287	**210**	166	190	218
FeAl (B2)	*2.812*	**2.869**	2.843	2.903	*208*	***180***	*193*	136
CoAl (B2)	2.795	**2.853**	2.826	2.861	207	**179**	192	162
NiAl (B2)	2.834	**2.894**	2.866	2.887	185	**159**	171	156
BN (B3)	3.585	3.629	**3.610**	3.616	405	**373**	387	369
BP (B3)	4.496	**4.553**	**4.526**	4.538	**176**	162	**170**	173
BAs (B3)	4.740	4.816	**4.778**	4.777	148	132	141	
AlN (B3)	4.346	4.406	**4.379**	4.38	211	193	**201**	202
AlP (B3)	5.440	5.513	**5.474**	5.463	89.9	82.6	**87.1**	86
AlAs (B3)	5.636	5.734	**5.680**	5.661	**75.5**	67.0	72.5	82
GaN (B3)	4.463	4.551	**4.504**	4.523	204	173	**190**	190
GaP (B3)	5.401	5.514	**5.448**	5.451	**90.6**	77.0	**85.5**	88
GaAs (B3)	5.616	5.757	**5.672**	5.648	**74.7**	61.0	69.5	75.6
InN (B3)	4.952	5.055	**4.997**	4.98	149	122	138	
InP (B3)	5.839	5.968	**5.890**	5.869	**72.0**	59.9	67.4	72
InAs (B3)	**6.038**	6.195	6.100	6.058	60.7	48.8	**56.6**	58
SiC (B3)	4.333	4.384	**4.360**	4.358	**230**	212	**221**	225
BN (B_k)	2.494	2.515	**2.507**	2.504				
CeO_2 (C1)	5.371	5.475	**5.415**	5.411	**209**	176	195	220
$MoSe_2$ (C7)	3.253	3.326	**3.284**	3.289				
me	−0.072	0.032	−0.016		22.3	−5.0	9.4	
mae	0.072	0.043	0.031		24.2	14.9	15.6	
mre	−1.66	0.65	−0.42		14.8	−4.1	4.4	
mare	1.66	0.92	0.71		16.2	10.3	10.0	

[a]Reference 11 for Li, C(A4), Na, Si, K, Ge, Rh, Pd, Ag, LiF, LiCl, NaF, NaCl, MgO, GaAs, and SiC; Ref. 73 for C(A9); Ref. 74 for Al, Cu, Ta, W, Pt, and Au; Ref. 75 for Ca, V, Sr, Nb, Mo, Ba, and Ir; Ref. 76 for Fe and Ni; Ref. 77 for Rb; Ref. 78 for Sn, BP (B_0), AlP (B_0), AlAs (B_0), GaP (B_0), InN, InP (B_0), and InAs (B_0); Ref. 79 for Th (a_0); Ref. 80 for Th (B_0); Ref. 81 for TiC; Ref. 82 for VC, ZrC, NbC, HfC, TiN, ZrN (a_0), and HfN (a_0); Ref. 83 for ScN, VN, YN, NbN (a_0), and LaN; Ref. 84 for ZrN (B_0), NbN (B_0), and HfN (B_0); Ref. 85 for CaO; Ref. 86 for MgS; Ref. 87 for MnO (a_0); Ref. 88 for MnO (B_0); Ref. 89 for FeO (a_0); Ref. 90 for FeO (B_0); Ref. 91 for CoO (a_0); Ref. 92 for CoO (B_0); Ref. 93 for NiO (a_0); Ref. 94 for NiO (B_0); Ref. 95 for ZnO; Ref. 96 for FeAl; Ref. 97 for CoAl; Ref. 98 for NiAl; Ref. 14 for BN(B3) (a_0), BP (a_0), BAs, AlP (a_0), AlAs (a_0), GaN (a_0), GaP (a_0), InP (a_0), and InAs (a_0); Ref. 99 for BN(B3) (B_0), AlN, and GaN (B_0); Ref. 100 for BN (B_k); Ref. 101 for CeO_2; and Ref. 102 for $MoSe_2$.

TABLE IX. Equilibrium lattice constant (in Å, a_0 for Ne, Ar, Kr, and Xe and c_0 for C, BN, and $MoSe_2$) whose value is determined by weak interactions. The Strukturbericht symbols (in parentheses) are used for the structure as follows: A1, fcc; A9, B_k, and C7, hexagonal structures. The best theoretical values are in boldface.

Solid	LDA	PBE	WC	Expt.
Ne (A1)	3.87	**4.6**	4.9	4.47[a]
Ar (A1)	**4.94**	6.0	6.4	5.31[a]
Kr (A1)	**5.33**	6.4	6.9	5.65[a]
Xe (A1)	**5.85**	7.1	7.6	6.13[a]
C (A9)	**6.64**	8.8	9.7	6.71[b]
BN (B_k)	**6.47**	8.4	7.2	6.66[c]
$MoSe_2$ (C7)	**12.77**	15.1	13.2	12.93[d]
me	−0.28	1.2	1.1	
mae	0.28	1.2	1.1	
mre	−5.1	17.0	18.5	
mare	5.1	17.0	18.5	

[a]References 103–105.
[b]Reference 73.
[c]Reference 100.
[d]Reference 102.

The calculated values for the bulk modulus (also shown in Table VIII) follow the usual trend: if a functional yields a lattice constant a_0 that is larger (smaller) than that of another functional, then the reverse will be the case for the bulk modulus B_0. This means that for most solids, the WC value for the bulk modulus is between the LDA and PBE values (except for some weakly bound solids, e.g., the rare-gas solids, for which we do not consider the bulk modulus). Nevertheless, concerning the comparison with the experimental values, there can be slight changes for some types of solids. For instance, for the three heaviest 5*d* transition metals, the WC functional is the best, while for the group-III-V compounds, LDA is as good as WC for the prediction of the bulk modulus. Overall, for the me and mre, PBE is better than the LDA and WC functionals, but if the mae and mare are considered, PBE and WC performances are similar with ~15 GPa for the mae and ~10% for the mare.

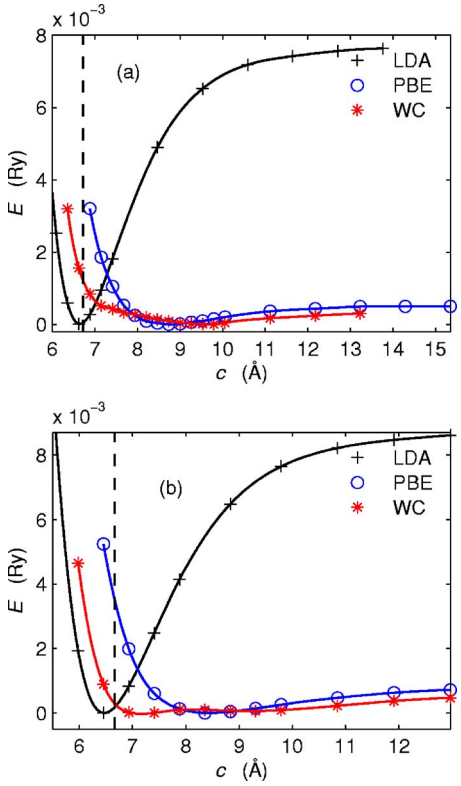

FIG. 3. (Color online) Graphite (a) and h-BN (b) total energies plotted as a function of the interlayer distance *c*. The vertical dashed line corresponds to the experimental value.

IV. CONCLUSIONS

We have presented results obtained with the new GGA exchange-correlation energy functional of Wu and Cohen,[16] and have compared its performance with other functionals. The length of covalent bonds in molecules is slightly better described by the WC functional, but the results on atomization energies are less accurate with WC than with PBE. WC has the tendency to give atomization energies larger than the PBE values, which were already too large. This is in agreement with the results of Wu and Cohen, who showed that the cohesive energies of solids are larger with the WC functional than with PBE. For noncovalent interactions, PBE remains the best functional, and it will be probably very difficult to find a better GGA functional than PBE because, compared to many other functionals (LDA, GGA, meta-GGA, hybrid, and meta-GGA-hybrid), it belongs to the group of the (very) best ones for most types of noncovalent interactions.[46]

The results on bulk solids show that the WC functional shows overall the best performance for the lattice constant. Except for Li and Na, the WC results are always between LDA and PBE, but not necessarily simply a "mean" value of them. Therefore, it can weaken (but by far not solve) the well-known problem that in most cases PBE is much better for "light" elements than for "heavy" ones. Unfortunately, it shows no improvement in breaking the well-known trends within a transition-metal series, where from left to right the error $a_0^{\text{calc}} - a_0^{\text{expt}}$ shifts in the direction of the positive values. The WC functional is best for group-I elements (including their ionic compounds), for group IV, for the III-V semiconductors, and for the 4*d* and (lighter) 5*d* elements and their compounds. In particular, it is *never* the "worst" functional of the three tested ones. PBE remains superior for group-II elements (although not for their oxides) and the 3*d* metals including their compounds and alloys. LDA remains the best functional not only for very heavy 5*d* elements but also for "weak interactions" as found in rare-gas solids and for the interlayer coupling of some layered materials. For surfaces, WC shows improvement over LDA and PBE for the surface formation energy for 3*d* transition-metal elements, while LDA is still the best for 4*d* and 5*d* elements.

Concerning the relation between the analytical forms (derived to recover the homogeneous electron gas and satisfy mathematical relations) and the performances of the tested functionals, a few observations can be made: the fact that in

most cases the WC results are situated between the LDA and PBE results was expected by looking at Fig. 1, where we can see that the WC enhancement factor $F(s)$ is below the PBE one, i.e., closer to LDA $[F^{\mathrm{LDA}}(s)=1]$. As discussed above, this makes WC better than LDA and PBE for the geometrical parameters of many of the solids we considered, but not for the thermochemistry of the covalently bound molecules. Another observation is that the different forms of the function $F(s)$ of the PW91 and PBE functionals for large values of s lead to differences in the energies, which are important for the very weakly bound systems (e.g., rare-gas dimers). The importance of the behavior of $F(s)$ for large values of s for noncovalent interactions was already pointed out in Refs. 36 and 37. More difficult to explain without a deeper analysis are the results obtained on the van der Waals systems (and a few other systems such as Li_2 and solid Li), which clearly show the trend of the WC functional to bind less (and to give larger interatomic distances) than the PBE functional does, despite the fact that $F^{\mathrm{WC}}(s)<F^{\mathrm{PBE}}(s)$ for $s>0$.

Overall, none of the functionals we have tested can be considered better than the others in all cases, but the observed trends among the different types of interactions and groups of atoms will certainly be very helpful for applications performed with LDA or GGA functionals.

ACKNOWLEDGMENTS

This work was supported by the AURORA Project No. SFB011 of the Austrian Science Fund, the Austrian Grid (WP A-7), and the EU (FP6-013817) "nanomesh" project. One of the authors (F.T.) is grateful for the support from the Swiss National Science Foundation (Grant No. PBGE2-108846).

[1] W. Kohn and L. J. Sham, Phys. Rev. **140**, A1133 (1965).
[2] P. Hohenberg and W. Kohn, Phys. Rev. **136**, B864 (1964).
[3] *Encyclopedia of Computational Chemistry*, edited by P. v. R. Schleyer, N. L. Allinger, T. Clark, J. Gasteiger, P. Kollman, H. F. Schaefer III, and P. R. Schreiner (Wiley, Chichester, 1998).
[4] S. Goedecker and G. E. Scuseria, Comput. Sci. Eng. **5**, 14 (2003).
[5] A. D. Becke, J. Chem. Phys. **98**, 1372 (1993).
[6] A. D. Becke, J. Chem. Phys. **98**, 5648 (1993).
[7] J. P. Perdew, S. Kurth, A. Zupan, and P. Blaha, Phys. Rev. Lett. **82**, 2544 (1999); **82**, 5179(E) (1999).
[8] S. Kurth, J. P. Perdew, and P. Blaha, Int. J. Quantum Chem. **75**, 889 (1999).
[9] J. Tao, J. P. Perdew, V. N. Staroverov, and G. E. Scuseria, Phys. Rev. Lett. **91**, 146401 (2003).
[10] V. N. Staroverov, G. E. Scuseria, J. Tao, and J. P. Perdew, J. Chem. Phys. **119**, 12129 (2003); **121**, 11507 (2004).
[11] V. N. Staroverov, G. E. Scuseria, J. Tao, and J. P. Perdew, Phys. Rev. B **69**, 075102 (2004).
[12] F. Corà, M. Alfredsson, G. Mallia, D. S. Middlemiss, W. C. Mackrodt, R. Dovesi, and R. Orlando, Struct. Bonding (Berlin) **113**, 171 (2004).
[13] J. Heyd and G. E. Scuseria, J. Chem. Phys. **121**, 1187 (2004).
[14] J. Heyd, J. E. Peralta, G. E. Scuseria, and R. L. Martin, J. Chem. Phys. **123**, 174101 (2005).
[15] J. Paier, M. Marsman, K. Hummer, G. Kresse, I. C. Gerber, and J. G. Ángyán, J. Chem. Phys. **124**, 154709 (2006); **125**, 249901 (2006).
[16] Z. Wu and R. E. Cohen, Phys. Rev. B **73**, 235116 (2006).
[17] J. P. Perdew, K. Burke, and M. Ernzerhof, Phys. Rev. Lett. **77**, 3865 (1996); **78**, 1396(E) (1997).
[18] V. I. Anisimov, J. Zaanen, and O. K. Andersen, Phys. Rev. B **44**, 943 (1991).
[19] F. Tran, P. Blaha, K. Schwarz, and P. Novák, Phys. Rev. B **74**, 155108 (2006).
[20] R. Kevorkyants, M. Dulak, and T. A. Wesolowski, J. Chem. Phys. **124**, 024104 (2006).
[21] E. R. Johnson and A. D. Becke, J. Chem. Phys. **124**, 174104 (2006).
[22] A. Puzder, M. Dion, and D. C. Langreth, J. Chem. Phys. **124**, 164105 (2006).
[23] F. Ortmann, F. Bechstedt, and W. G. Schmidt, Phys. Rev. B **73**, 205101 (2006).
[24] J. P. Perdew, J. Tao, V. N. Staroverov, and G. E. Scuseria, J. Chem. Phys. **120**, 6898 (2004).
[25] P. A. M. Dirac, Proc. Cambridge Philos. Soc. **26**, 376 (1930).
[26] S. H. Vosko, L. Wilk, and M. Nusair, Can. J. Phys. **58**, 1200 (1980).
[27] J. P. Perdew and Y. Wang, Phys. Rev. B **45**, 13244 (1992).
[28] D. M. Ceperley and B. J. Alder, Phys. Rev. Lett. **45**, 566 (1980).
[29] J. P. Perdew, J. A. Chevary, S. H. Vosko, K. A. Jackson, M. R. Pederson, D. J. Singh, and C. Fiolhais, Phys. Rev. B **46**, 6671 (1992); **48**, 4978(E) (1993).
[30] P. S. Svendsen and U. von Barth, Phys. Rev. B **54**, 17402 (1996).
[31] Y. Zhang and W. Yang, Phys. Rev. Lett. **80**, 890 (1998).
[32] B. Hammer, L. B. Hansen, and J. K. Nørskov, Phys. Rev. B **59**, 7413 (1999).
[33] C. Adamo and V. Barone, J. Chem. Phys. **116**, 5933 (2002).
[34] X. Xu and W. A. Goddard III, J. Chem. Phys. **121**, 4068 (2004).
[35] G. K. H. Madsen, cond-mat/0609365, Phys Rev. B (to be published).
[36] T. A. Wesolowski, O. Parisel, Y. Ellinger, and J. Weber, J. Phys. Chem. A **101**, 7818 (1997).
[37] Y. Zhang, W. Pan, and W. Yang, J. Chem. Phys. **107**, 7921 (1997).
[38] A. St-Amant and D. R. Salahub, Chem. Phys. Lett. **169**, 387 (1990); A. St-Amant, Ph.D. thesis, University of Montreal, 1992; M. E. Casida, C. Daul, A. Goursot, A. Koester, L. G. M. Pettersson, E. Proynov, A. St-Amant, and D. R. Salahub, S. Chrétien, H. Duarte, N. Godbout, J. Guan, C. Jamorski, M. Leboeuf, V. Malkin, O. Malkina, M. Nyberg, L. Pedocchi, F. Sim, and A. Vela, DEMON-KS, Version 3.5, deMon Software, 1998.
[39] H. Partridge, J. Chem. Phys. **87**, 6643 (1987).
[40] H. Partridge, J. Chem. Phys. **90**, 1043 (1989).
[41] S. F. Boys and F. Bernardi, Mol. Phys. **19**, 553 (1970).
[42] N. Godbout, D. R. Salahub, J. Andzelm, and E. Wimmer, Can. J. Chem. **70**, 560 (1992).
[43] P. Blaha, K. Schwarz, G. K. H. Madsen, D. Kvasnicka, and J. Luitz, *WIEN2K: An Augmented Plane Wave and Local Orbitals*

Program for Calculating Crystal Properties, edited by K. Schwarz (Vienna University of Technology, Vienna, Austria, 2001).
[44] J. L. F. Da Silva, C. Stampfl, and M. Scheffler, Surf. Sci. **600**, 703 (2006).
[45] X. Xu, Q. Zhang, R. P. Muller, and W. A. Goddard III, J. Chem. Phys. **122**, 014105 (2005).
[46] Y. Zhao and D. G. Truhlar, J. Chem. Theory Comput. **1**, 415 (2005).
[47] Y. Zhao and D. G. Truhlar, J. Phys. Chem. A **109**, 5656 (2005).
[48] D. Cappelletti, M. Bartolomei, F. Pirani, and V. Aquilanti, J. Phys. Chem. A **106**, 10764 (2002).
[49] J. F. Ogilvie and F. Y. H. Wang, J. Mol. Struct. **273**, 277 (1992).
[50] J. F. Ogilvie and F. Y. H. Wang, J. Mol. Struct. **291**, 313 (1993).
[51] M. O. Sinnokrot, E. F. Valeev, and C. D. Sherrill, J. Am. Chem. Soc. **124**, 10887 (2002).
[52] A. D. Boese and J. M. L. Martin, J. Chem. Phys. **121**, 3405 (2004).
[53] A. E. Mattsson, R. Armiento, P. A. Schultz, and T. R. Mattsson, Phys. Rev. B **73**, 195123 (2006).
[54] S. Tsuzuki and H. P. Lüthi, J. Chem. Phys. **114**, 3949 (2001).
[55] M. D. Patey and C. E. H. Dessent, J. Phys. Chem. A **106**, 4623 (2002).
[56] M. O. Sinnokrot and C. D. Sherrill, J. Phys. Chem. A **108**, 10200 (2004).
[57] D. C. Patton and M. R. Pederson, Phys. Rev. A **56**, R2495 (1997); **71**, 019906(E) (2005).
[58] D. C. Patton and M. R. Pederson, Int. J. Quantum Chem. **69**, 619 (1998).
[59] T. van Mourik and R. J. Gdanitz, J. Chem. Phys. **116**, 9620 (2002).
[60] J. Tao and J. P. Perdew, J. Chem. Phys. **122**, 114102 (2005).
[61] Y. Zhao and D. G. Truhlar, J. Phys. Chem. A **110**, 5121 (2006).
[62] J. Ireta, J. Neugebauer, and M. Scheffler, J. Phys. Chem. A **108**, 5692 (2004).
[63] M. Hasegawa and K. Nishidate, Phys. Rev. B **70**, 205431 (2004).
[64] G. B. Grad, P. Blaha, K. Schwarz, W. Auwärter, and T. Greber, Phys. Rev. B **68**, 085404 (2003).
[65] L. Vitos, A. V. Ruban, H. L. Skriver, and J. Kollár, Surf. Sci. **411**, 186 (1998).
[66] W. R. Tyson and W. A. Miller, Surf. Sci. **62**, 267 (1977).
[67] F. R. de Boer, R. Boom, W. C. M. Mattens, A. R. Miedema, and A. K. Niessen, in *Cohesion in Metals: Transition Metal Alloys*, edited by F. R. de Boer and D. G. Pettifor (North-Holland, Amsterdam, 1988), Vol. 1.
[68] A. Nagashima, N. Tejima, Y. Gamou, T. Kawai, and C. Oshima, Phys. Rev. B **51**, 4606 (1995).
[69] M. Morscher, M. Corso, T. Greber, and J. Osterwalder, Surf. Sci. **600**, 3280 (2006).
[70] M. Corso, W. Auwärter, M. Muntwiler, A. Tamai, T. Greber, and J. Osterwalder, Science **303**, 217 (2004).
[71] A. B. Preobrajenski, A. S. Vinogradov, and N. Mårtensson, Surf. Sci. **582**, 21 (2005).
[72] A. B. Preobrajenski, A. S. Vinogradov, E. Cávar, R. Westerström, A. Mikkelsen, E. Lundgren, and N. Mårtensson (unpublished).
[73] P. Trucano and R. Chen, Nature (London) **258**, 136 (1975).
[74] A. Dewaele, P. Loubeyre, and M. Mezouar, Phys. Rev. B **70**, 094112 (2004).
[75] M. J. Mehl and D. A. Papaconstantopoulos, Phys. Rev. B **54**, 4519 (1996).
[76] F. Starrost, H. Kim, S. C. Watson, E. Kaxiras, and E. A. Carter, Phys. Rev. B **64**, 235105 (2001).
[77] P. Legrand and F. Perrot, J. Phys.: Condens. Matter **13**, 287 (2001).
[78] S. Q. Wang and H. Q. Ye, Phys. Rev. B **66**, 235111 (2002).
[79] D. S. Evans and G. V. Raynor, J. Nucl. Mater. **1**, 281 (1959).
[80] G. Bellussi, U. Benedict, and W. B. Holzapfel, J. Less-Common Met. **78**, 147 (1981).
[81] M. Guemmaz, A. Mosser, R. Ahujab, and B. Johansson, Solid State Commun. **110**, 299 (1999).
[82] E. I. Isaev, R. Ahuja, S. I. Simak, A. I. Lichtenstein, Yu. Kh. Vekilov, B. Johansson, and I. A. Abrikosov, Phys. Rev. B **72**, 064515 (2005).
[83] C. Stampfl, W. Mannstadt, R. Asahi, and A. J. Freeman, Phys. Rev. B **63**, 155106 (2001).
[84] X.-J. Chen, V. V. Struzhkin, Z. Wu, M. Somayazulu, J. Qian, S. Kung, A. N. Christensen, Y. Zhao, R. E. Cohen, H.-K. Mao, and R. J. Hemley, Proc. Natl. Acad. Sci. U.S.A. **102**, 3198 (2005).
[85] P. Richet, H.-K. Mao, and P. M. Bell, J. Geophys. Res. **93**, 15279 (1988).
[86] S. M. Peiris, A. J. Campbell, and D. L. Heinz, J. Phys. Chem. Solids **55**, 413 (1994).
[87] R. W. G. Wyckoff, *Crystal Structures* (Interscience, New York, 1964).
[88] Y. Noguchi, K. Kusaba, K. Fukuoka, and Y. Syono, Geophys. Res. Lett. **23**, 1469 (1996).
[89] C. A. McCammon and L.-G. Liu, Phys. Chem. Miner. **10**, 106 (1984).
[90] S. D. Jacobsen, H.-J. Reichmann, H. A. Spetzler, S. J. Mackwell, J. R. Smyth, R. J. Angel, and C. A. McCammon, J. Geophys. Res. **107**, 2037 (2002).
[91] M. J. Carey, F. E. Spada, A. E. Berkowitz, W. Cao, and G. Thomas, J. Mater. Res. **6**, 2680 (1991).
[92] Q. Guo, H.-K. Mao, J. Hu, J. Shu, and R. J. Hemley, J. Phys.: Condens. Matter **14**, 11369 (2002).
[93] L. C. Bartel and B. Morosin, Phys. Rev. B **3**, 1039 (1971).
[94] E. Huang, K. Jy, and S.-C. Yu, J. Geophys. Soc. China **37**, 7 (1994).
[95] F. Decremps, F. Datchi, A. M. Saitta, A. Polian, S. Pascarelli, A. Di Cicco, J. P. Itié, and F. Baudelet, Phys. Rev. B **68**, 104101 (2003).
[96] L. Shaojun, D. Suqing, and M. Benkun, Phys. Rev. B **58**, 9705 (1998).
[97] S. Öğüt and K. M. Rabe, Phys. Rev. B **50**, 2075 (1994).
[98] P. A. Korzhavyi, A. V. Ruban, A. Y. Lozovoi, Yu. Kh. Vekilov, I. A. Abrikosov, and B. Johansson, Phys. Rev. B **61**, 6003 (2000).
[99] H. M. Tütüncü, S. Bağci, G. P. Srivastava, A. T. Albudak, and G. Uğur, Phys. Rev. B **71**, 195309 (2005).
[100] R. S. Pease, Acta Crystallogr. **5**, 356 (1952).
[101] L. Gerward, J. Staun Olsen, L. Petit, G. Vaitheeswaran, V. Kanchana, and A. Svane, J. Alloys Compd. **400**, 56 (2005).
[102] K. D. Bronsema, J. L. de Boer, and F. Jellinek, Z. Anorg. Allg. Chem. **540**, 15 (1986).
[103] M. S. Anderson, R. Q. Fugate, and C. A. Swenson, J. Low Temp. Phys. **10**, 345 (1973).
[104] M. S. Anderson and C. A. Swenson, J. Phys. Chem. Solids **36**, 145 (1975).
[105] T. Tsuchiya and K. Kawamura, J. Chem. Phys. **117**, 5859 (2002).